Effects of Spectral Error in Efficiency Measurements of GaInAs-Based Concentrator Solar Cells

C.R. Osterwald, M.W. Wanlass, T. Moriarty, M.A. Steiner, and K.A. Emery

Effects of Spectral Error in Efficiency Measurements of GaInAs-Based Concentrator Solar Cells

C.R. Osterwald, M.W. Wanlass, T. Moriarty, M.A. Steiner, and K.A. Emery

Prepared under Task No. PV13.1010

NOTICE

This report was prepared as an account of work sponsored by an agency of the United States government. Neither the United States government nor any agency thereof, nor any of their employees, makes any warranty, express or implied, or assumes any legal liability or responsibility for the accuracy, completeness, or usefulness of any information, apparatus, product, or process disclosed, or represents that its use would not infringe privately owned rights. Reference herein to any specific commercial product, process, or service by trade name, trademark, manufacturer, or otherwise does not necessarily constitute or imply its endorsement, recommendation, or favoring by the United States government or any agency thereof. The views and opinions of authors expressed herein do not necessarily state or reflect those of the United States government or any agency thereof.

Abstract

This technical report documents a particular error in efficiency measurements of triple-absorber concentrator solar cells caused by incorrect spectral irradiance—specifically, one that occurs when the irradiance from unfiltered, pulsed xenon solar simulators into a GaInAs bottom subcell is too high. For cells designed so that the light-generated photocurrents in the three subcells are nearly equal, this condition can cause a large increase in the measured fill factor, which, in turn, causes a significant artificial increase in the efficiency. The error is readily apparent when the data under concentration are compared to measurements with correctly balanced photocurrents, and manifests itself as discontinuities in plots of fill factor and efficiency versus concentration ratio. In this work, we simulate the magnitudes and effects of this error with a device-level model of two concentrator cell designs, and demonstrate how a new Spectrolab, Inc., Model 460 Tunable-High Intensity Pulsed Solar Simulator (T-HIPSS) can mitigate the error. Although in this work the error has been identified in GaInAs bottom subcells, increasing the photocurrent in any subcell will produce similar errors, regardless of the chemical composition.

Acknowledgment

List of Symbols and Acronyms

1-sun	total solar irradiance of 1000 Wm^{-2}
A	PV device total area
E	total solar irradiance
HIPSS	high intensity pulsed solar simulator
I-V	PV device current versus voltage curve
I_{sc}	short-circuit current
FF	fill factor
M	spectral mismatch parameter
N	number of subcells in a multijunction solar cell
n	solar cell diode quality factor
NREL	National Renewable Energy Laboratory
OSMSS	one-sun multisource solar simulator
P_{max}	maximum power
R	photocurrent ratio
PV	photovoltaics
QE	quantum efficiency
SRC	standard reporting conditions
T-HIPSS	tunable-high intensity pulsed solar simulator
$\times$	concentration ratio
V_{oc}	open-circuit voltage
η	solar cell power efficiency
ρ	solar cell photocurrent

List of Figures

Table of Contents

1 Introduction

The electrical performance of solar photovoltaic (PV) cells and modules is strongly affected by the incident light, both the overall intensity level (i.e. the total irradiance) and its variation over wavelength. Standard measurements of solar PV device performance require that electrical efficiency be determined with respect to reference spectral irradiance distributions, which are tables of solar irradiance and light wavelength pairs [1,2]. A reference spectrum is one element of standard reporting conditions (SRC), which also specify the total irradiance and the internal PV cell operating temperature. Electrical performance is measured by tracing the current-voltage (I-V) curve of a device while it is illuminated [3-6].

While these tables, which are generated by computer models, cannot represent how the light from the sun changes over time, they are the only consistent basis on which the performance of different solar cells can be compared. For modules, performance measurements at SRC are now so institutionalized in the PV industry that the power at 25°C, a total irradiance of 1000 Wm^{-2} and the global reference spectrum [1] is deemed the "peak-watt rating", even though a module will likely never operate under these exact conditions. This total irradiance is defined as 1-sun.

Power, the product of current and voltage, is highest on the I-V curve at the maximum-power point, P_{max}, and PV efficiency is defined as:

$$\eta = \frac{P_{max}}{E \cdot A} \tag{1}$$

In Eq. 1, E is the total irradiance and A is the total area of the device. Three other important I-V curve parameters are the short-circuit current (I_{sc}), the open-circuit voltage (V_{oc}), and the fill factor (FF), which are related by:

$$FF = \frac{P_{max}}{I_{sc} \cdot V_{oc}} \tag{2}$$

Determination of efficiency at SRC obviously requires the test device to be illuminated with the desired reference spectrum, but exact reproduction of a given solar spectrum is impossible, even outdoors in real sunlight. Approximations can be made with solar simulators using Xe arc lamps. For cells fabricated with a single semiconductor absorber, such as CdTe or crystalline Si, illumination with an incorrect spectrum produces an error in the measured current when the total irradiance is measured with a calibrated reference cell. Knowing the relative spectral response (or equivalently, the quantum efficiency, QE) of the test device and the simulator spectrum, the error can be mitigated using the spectral mismatch parameter, M [3-7].

1

1.1 Multijunction Efficiency Measurements

More complicated PV devices have multiple semiconductor subcells stacked on top of each other and electrically connected in series[1]. Light enters the top subcell of these multijunction devices and passes through to deeper subcells, minus the light absorbed in higher subcells. The light absorbed in each subcell causes the generation of unique internal photocurrents. These photocurrents each produce a voltage across the corresponding subcell that add to produce a higher voltage as compared to a single absorber device. Because the subcells are series-connected, the same current must flow through all the subcells, even if the photocurrents are not identical.

Under illumination, each subcell has a particular I-V curve that is a function of its photocurrent. However, independent measurement of these I-V curves is not possible because a multijunction solar cell has just two electrical terminals. The subcell internal I-V characteristics combine in a non-intuitive way to form the I-V curve of the solar cell that can be externally measured [8]. As a result, spectral content of light applied to multijunction devices affects not only the current but also the voltage and the shape (i.e. the fill factor, *FF*) of the measured I-V curve [9]. Thus, in order to accurately measure the performance of a multijunction device, it must be illuminated with light such that the photocurrents (ρ) correspond to those that would be produced by the reference spectrum. In general, photocurrent balancing (or tuning) must be done with a spectrally adjustable solar simulator [10-15].

Forming the ratios of the photocurrents (*R*) of every subcell with all other subcells is a way to map the photocurrent balance for any given spectrum. The *R* values correspond to the ratios of the effective irradiances impinging the subcells. The number of ratios needed is the mathematical combination of *N* subcells taken 2 at a time, or:

$$C(N,2) = \frac{N!}{(N-2)!} = 1, 3, 6, 10, 15\ldots, \text{ for } N = 2, 3, 4, 5, 6\ldots \tag{3}$$

An iterative adjustment procedure can be used in which photocurrent ratios are measured with calibrated reference cells that correspond to each subcell (also known as isotype reference cells) and the simulator spectrum is measured with an instrument called a spectroradiometer or spectrometer. Because the subcell photocurrents cannot be measured directly, they are instead inferred from the reference cell I_{sc} values, modified by the spectral mismatch [14,15]. The ratios of the inferred photocurrents are compared, the spectrum is altered, and the process repeated until all ratios are sufficiently close to one.

Ideally, to facilitate the iterative procedure, the number of adjustable simulator parameters needed for testing any given multijunction device should be equal to *N*, with each parameter corresponding to the spectral regions of the individual subcells. If an adjustment alters the photocurrents of multiple subcells, the iteration is more difficult because more photocurrent ratios are changed.

---

[1] The word "junction" is commonly used to refer to one portion of a multijunction solar cell that absorbs a particular wavelength region. Because the series connections between the absorbers use semiconductor devices called tunneling *p-n* junctions, in this report we instead refer to the individual absorbers as "subcells" to avoid confusion.

2

Spectral tuning was first used for amorphous-Si cells with two and three subcells [10,11], and then later for high-efficiency group III-V solar cells [12], especially the GaInP/GaAs/Ge triple scheme [14]. For reference, Fig. 1 shows quantum efficiency (QE) versus wavelength plots that are representative of the subcells discussed in this report. For a single-absorber solar cell, I_{sc} is equal to a convolution over wavelength of its QE and the incident spectrum [3,4,7].
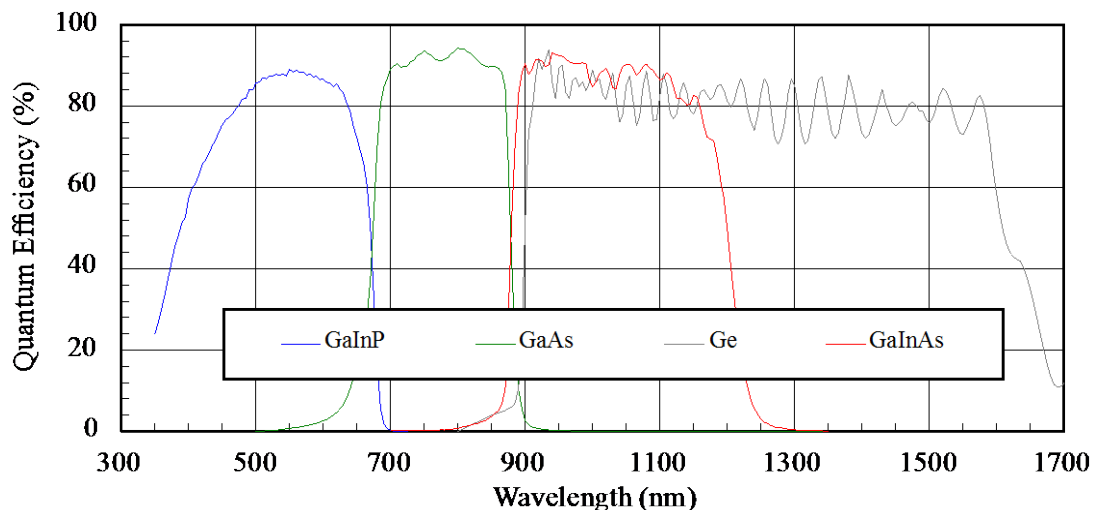
Figure 1. Example quantum efficiencies for subcells typically used for group III-V concentrator solar cells.

At NREL, multijunction performance measurements at SRC were first done in a Spectrolab, Inc. model X-25 Xe-arc simulator retrofitted with optical filters and apertures to subtract light in specific spectral regions. The iterative adjustment procedure could be quite tedious and time-consuming, often requiring a whole day, and is intractable for devices with more than three subcells [14].

In 2011 the X-25 procedure was replaced with a new instrument called the one-sun multisource solar simulator (OSMSS) that features nine separate light sources covering different wavelength regions. All nine sources can be independently adjusted from zero to 150% of 1-sun levels, and the spectral adjustment is completely automated [16]. The OSMSS has successfully measured devices with as many as six subcells.

1.2 Concentrator Cell Measurements

Concentrator cells take advantage of how solar cell efficiency increases as sunlight is focused onto smaller areas. As the total irradiance on a cell is increased, the current scales roughly linearly while the voltage increases logarithmically. The efficiency (proportional to voltage times current, see Eq. 1) also increases approximately logarithmically until losses (especially series resistance) cause it to decrease at higher concentration. Thus, a plot of efficiency versus irradiance will show a peak value at some value of irradiance.

Standard reporting conditions for concentrator cells are defined as the ASTM G173 direct reference spectrum [1], scaled to the desired concentration, and a cell temperature of 25°C. Although the G173 direct spectrum has a total irradiance of 900 Wm^{-2}, 1-sun is still defined as 1000 Wm^{-2}, which effectively scales the spectrum by 10:9 independently of wavelength [6,14].

3

Concentration is determined by assuming I_{sc} is directly proportional to irradiance (slight deviations from this assumption are neglected here). I_{sc} is measured at 1-sun and again under concentrated light; the ratio of the two is the concentration ratio, ×. Sunlight concentrated to 150×, for example, corresponds to 150 kWm^{-2}. Different cell designs have varying peak concentrations; the practical maximum concentration is about 2000×.

An important problem with efficiency measurements at SRC of concentrator cells is that the high irradiance levels cause heating, high enough to melt metallic materials. In a real system this means the design must include means to limit cell temperatures to acceptable levels using passive or active cooling. Indoor laboratory testing at SRC with the relatively cold temperature of 25°C dictates that temperature mitigation be done by restricting the illumination time using pulsed light sources. Commercial simulators have flash durations of a few milliseconds, so that if a test cell is mounted on a temperature-controlled block with good heat conduction, the temperature rise during the flash will be negligible.

2 Concentrator Efficiency Measurements at NREL

The NREL PV Cell and Module Performance Characterization Group has used two different commercial solar simulators for concentrator efficiency measurements with respect to SRC; these measurement systems are now described.

2.1 High Intensity Pulsed Solar Simulator (HIPSS)

NREL has used a Spectrolab, Inc. HIPSS for concentrator performance measurements since 1996 [14,17]. It features two long-arc Xe flash lamps with a total illumination time of 3 milliseconds; parabolic reflectors focus the light onto the test plane, which is about 1 meter below the lamps. A power supply called a pulse-forming network (PFN) charges a large capacitor to a setpoint of several thousand volts, then a high-voltage trigger initiates the flash discharge in the lamps. Spectrolab terms the trigger setpoint voltage divided by 10 the pulse network voltage (PNV). The flash irradiance is varied with the PNV and with adjustable slits in front of the lamps. To keep the lamp temperature constant, and thus also the spectral irradiance, the time between flashes should be a minimum of 1 to 2 minutes.

After an initial rise time, the irradiance is relatively stable for about 1 ms during which time the I-V curve is swept. An analog electronic load traces the I-V curve but can only sweep in one direction, from I_{sc} to V_{oc}. For unknown reasons, the load can oscillate when sweeping I-V curves on some cells, sometimes to a level where it is completely unable to sweep an I-V curve. The analog-to-digital converters for the current and voltage measurements are only 12-bit, which limits the resolution to 1 out of 4096. Another limitation of the HIPSS is a tendency to give unreliable data for concentration ratios below 10×.

The spectral irradiance of a flash depends on the PNV setting; as the lamp voltage increases the temperature of the Xe plasma increases. This has the affect of shifting the spectral irradiance toward shorter wavelengths less than 700 nm in the visible and ultraviolet regions.

Accurate measurements of the HIPSS's spectral irradiance have been problematic because of a lack of suitable spectroradiometers. A system was developed at NREL that measures spectral irradiance during a flash at a fixed wavelength [17]; because of this limitation, acquisition of an

4

entire spectrum requires many flashes and many hours of time. Thus, obtaining spectra for more than two PNV values is impractical. Figure 2 compares two measured HIPSS spectra, at different PNV values, against the direct reference spectrum.
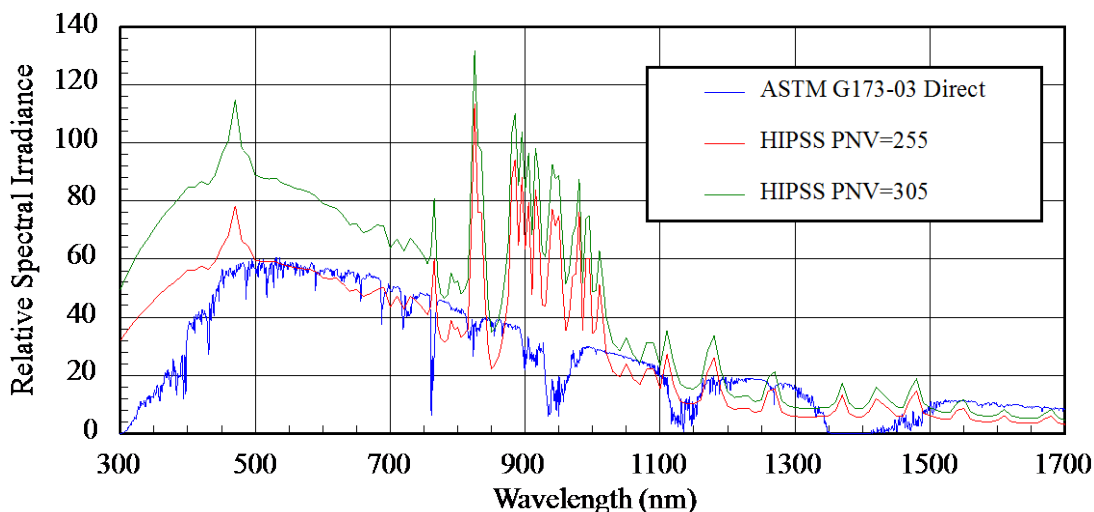

Figure 2. Relative spectral irradiance versus wavelength of the ASTM G173 direct reference spectrum and the NREL HIPSS for two different PNV settings.

The PNV is the only parameter available for adjusting the spectrum, and the lack of suitable spectral measurements precludes use of the iterative spectral adjustment procedure described previously. Despite these drawbacks, the HIPSS was the only available option for concentrator I-V measurements. For tandem cells such as GaInP/GaAs, the ratio of the GaInP top subcell photocurrent to that of the GaAs bottom subcell can be adjusted by changing the PNV. By assuming the spectrum changes linearly with PNV, a calculation was devised to select a suitable PNV based on the two measured spectra and the measured quantum efficiencies (QE) of the two junctions. The procedure adopted was:

- Measure the QE of each subcell [9-11,15]
- Calibrate the 1-sun I_{sc} of the cell in the X-25 using the iterative spectral adjustment
- Determine the HIPSS PNV setting to balance the top and bottom photocurrents
- Flash the cell repeatedly under the HIPSS; measure I-V curves as the irradiance is varied
- Divide the I_{sc} for each flash by the 1-sun I_{sc}
- Calculate the irradiance and concentration ratio
- Plot the I-V parameters versus log (concentration ratio) and locate the peak efficiency.

Figure 3 is an example of HIPSS data for a GaInP/GaAs tandem that includes the 1-sun I-V data point, which was measured with the X-25 spectrally adjusted according to the QEs of the two subcells. Because GaAs does not absorb wavelengths greater than 900 nm (compare Figs. 1 and 2), the simulator spectrum in the near infrared (IR) region is irrelevant. Each data point represents a separate flash and I-V curve. Note how all three curves match with the 1-sun values, and how the V_{oc} increases logarithmically.

5
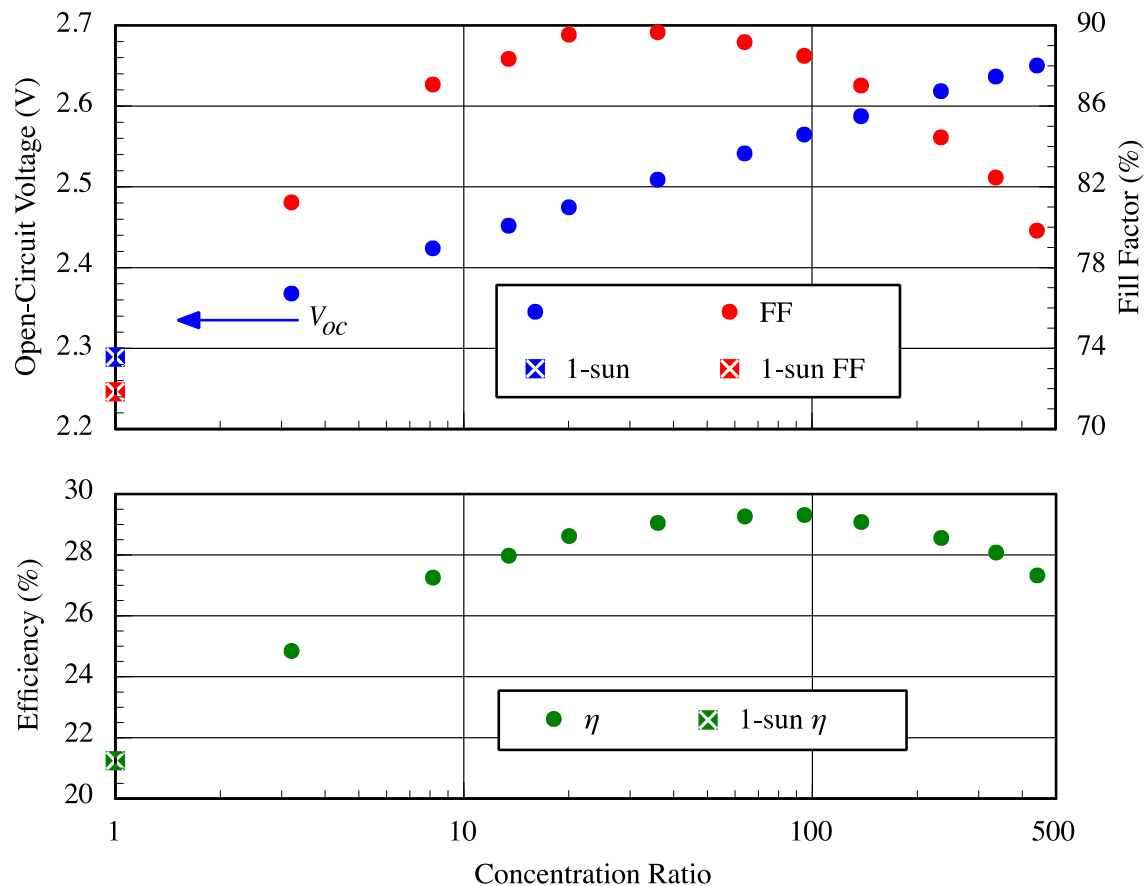
Figure 3. Open-circuit voltage, fill factor, and efficiency versus concentration ratio for a GaInP/GaAs tandem cell (HIPSS data).

This procedure was extended to GaInP/GaAs/Ge triple devices by considering the nature of the bottom Ge subcell, which absorbs light out to 1800 nm in the infrared and produces photocurrents that are 30-40% higher than the top and middle subcells. From this, two assumptions were made: 1) the external current through the entire cell under illumination will likely be limited by either the top or middle subcell, and 2) the exact photocurrent level in the bottom subcell is less important. Thus, the large number of Xe emission lines in the 800-1000 nm wavelength region of the HIPSS (Fig. 2) probably would not adversely affect results.

An example HIPSS measurement of a Ge-based triple cell is Fig. 4, in which the efficiency peaks at 41% when the concentration ratio is about 300×. The top-middle R was adjusted via the PNV setting of the simulator and the 1-sun measured with the X-25, as discussed above. Here again the V_{oc} increases logarithmically from the 1-sun point through about two decades of concentration ratio. Without the ability to adjust the spectral irradiance under concentration, verification of the PNV selection procedure has not been possible.

6
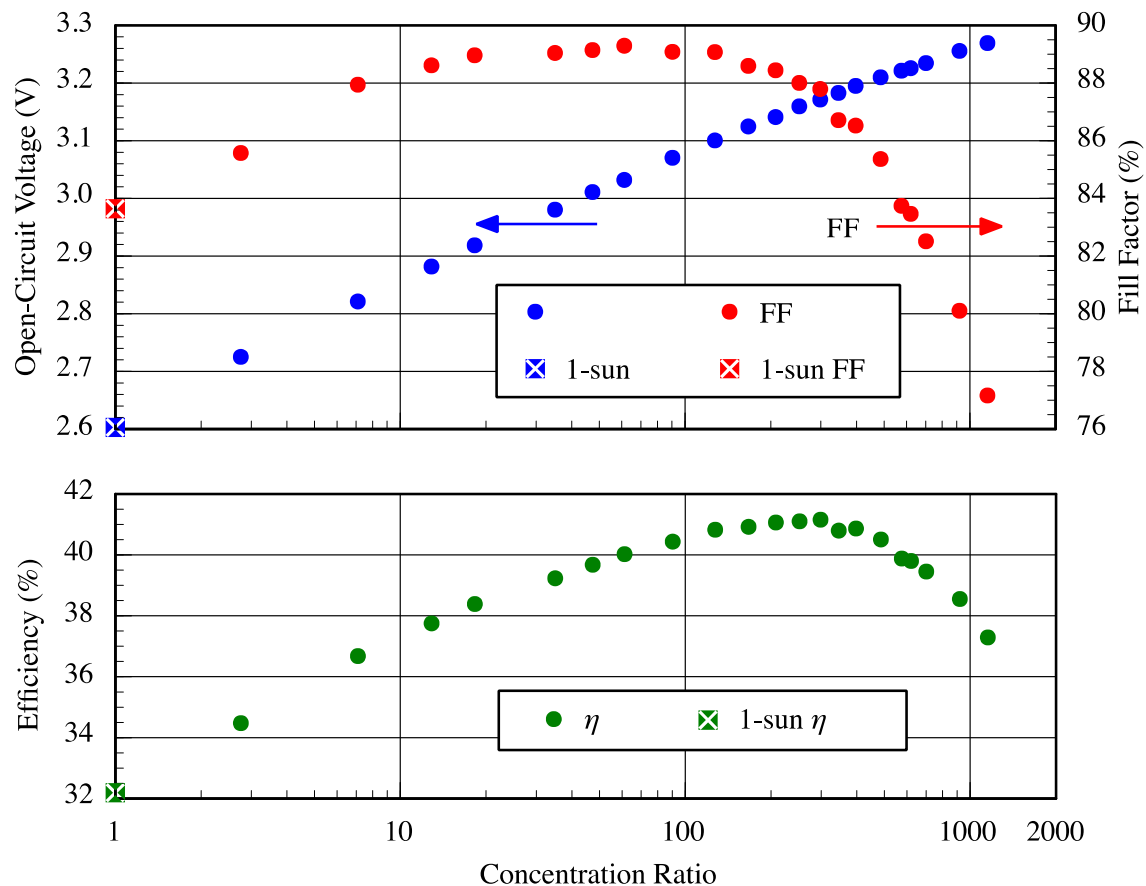
Figure 4. Open-circuit voltage, fill factor, and efficiency versus concentration ratio for a 41%-efficient GaInP/GaAs/Ge triple cell (HIPSS data).

2.2 Tunable-High Intensity Pulsed Solar Simulator (T-HIPSS)

The lack of a simulator with adjustable spectral content was certainly realized as a severe limitation for accurate concentrator cell measurements, and in 2008 NREL entered into a contract with Spectrolab to develop a suitable instrument. The defined requirements were quite ambitious, and included: 1) independent spectral adjustment in six wavelength bands from 400 to 1800 nm, 2) complete spectral irradiance measurement during a single flash, and 3) improved instrumentation for I-V curve measurements. Spectrolab's proposal was to develop an improved version of their existing Model 420 tunable-high intensity pulsed solar simulator (T-HIPSS) that would be coupled with a high-speed spectrometer (which was not available at the time) and completely new instrumentation (the Model 420 T-HIPSS has the same analog instrumentation as the HIPSS).

In 2013 Spectrolab completed development and delivered the Model 460 T-HIPSS; the instrument has now replaced the HIPSS for all standard concentrator cell efficiency measurements at NREL. The T-HIPSS still uses a PFN, but has a single Xe bulb design instead of the two-bulb HIPSS, and 14 discrete thin-film dielectric mirrors replace the parabolic reflectors. Spectral adjustment is accomplished with computer-controlled shutters that cover the mirrors, thus giving the ability to subtract light in six different wavelength bands (Fig. 5).

7
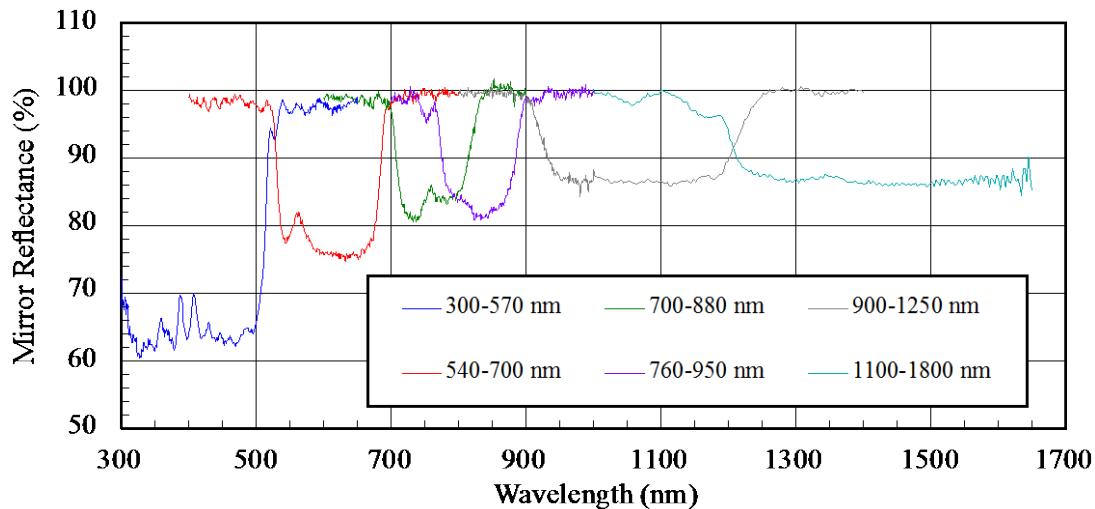
Figure 5. Spectral reflectance versus wavelength of the T-HIPSS Model 460 dielectric mirrors.

Other important features of the T-HIPSS include the state-of-the-art Avantes spectrometer, high-speed 16-bit analog-to-digital conversion, and programmable electronic loads that are able to sweep I-V curves in both directions. The loads are also well suited for measuring current at a fixed voltage, and can measure no-load V_{oc}.

3 GaInAs-Based Triple Cells

Development of improved concentrator cells has continued with the goal of ever-increasing efficiencies, which has increased the need for accurate measurements. The GaInP/GaAs/Ge structure has shown excellent results, 41% or greater for concentrator applications, and has supplanted Si for space power applications (in non-concentrating forms). Its theoretical efficiency limits, however, have dictated that research and development be directed toward replacing the Ge bottom subcell with a subcell having a more optimally current-matched ~1-eV bandgap. Several effective ways have been demonstrated to accomplish this, including the use of bottom subcells based on GaInAs-based compound semiconductors.[2]

From the performance measurements point-of-view, the most significant feature of these newer cells is that the photocurrents in all three subcells can be very close to each other. With its wider bandgap, GaInAs absorbs less light than Ge subcells (see Fig. 1) and therefore generates less current. However, such cells invalidate the assumptions made for HIPSS measurements that allowed for spectral adjustment based on the lamp voltage alone. If the photocurrent ratios deviate significantly from unity, additional error should be expected.

---

[2] The exact compositions of these semiconductors are unimportant for the purposes of this report.

3.1 Effects of Photocurrent Imbalance

By 2010 a significant number of GaInP/GaAs/GaInAs cells were being submitted to the Cell and Module Performance Characterization Group for concentrator measurement, and Fig. 6 is an example of HIPSS data. At first glance these data seem reasonable, but comparison with Figs. 3 and 4 shows an important difference—extrapolation of the trends down to 1× do not match the same values of V_{oc}, FF, and η as measured in the spectrally adjusted X-25. A ~3% relative discontinuity in η is evident, the V_{oc} is offset by 37 mV, and the FF is higher by 1 percentage point.
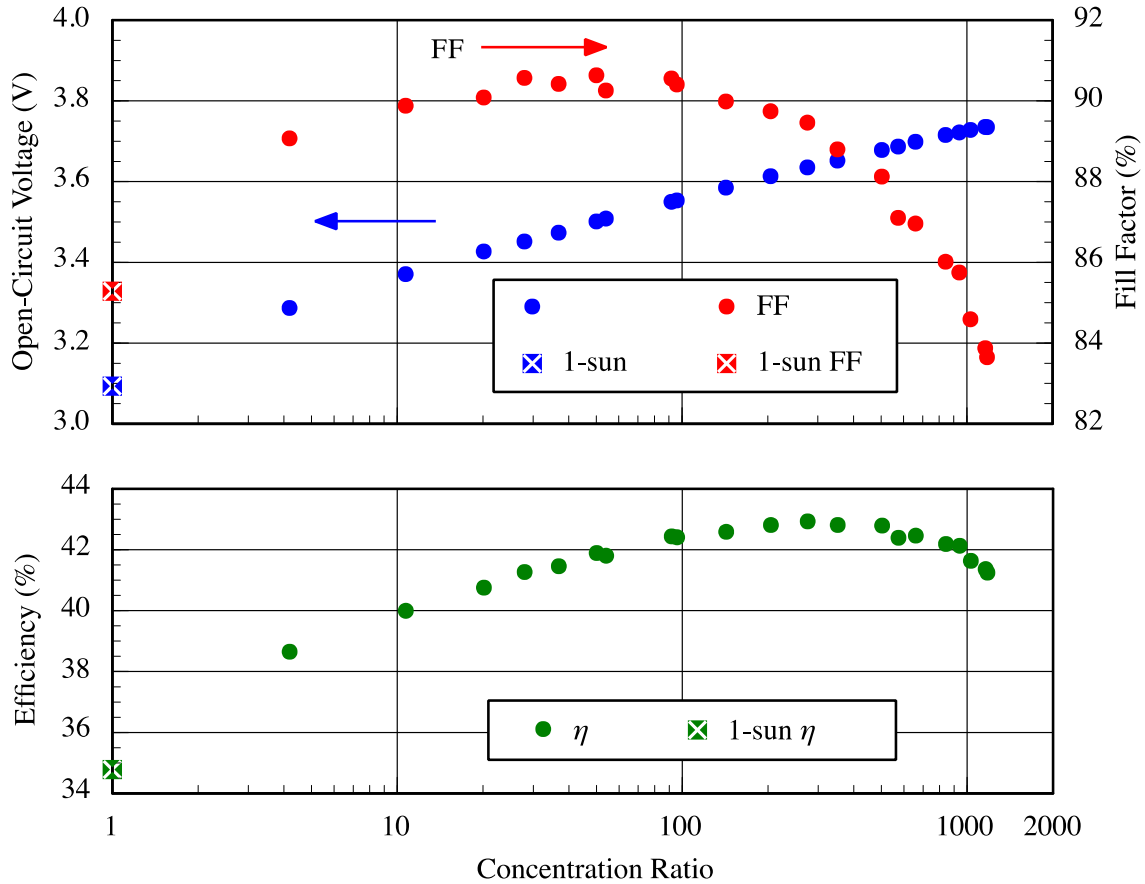

Figure 6. Open-circuit voltage, fill factor, and efficiency versus concentration ratio for a GaInP/GaAs/GaInAs triple cell (HIPSS data).

9

3.2 Excess Irradiance Estimation

Without measurements of the HIPSS spectral irradiance it is not possible to know the exact photocurrent ratios for Fig. 6, but the excess V_{oc} is an important clue to understanding what is happening. At open-circuit, no current is flowing through the cell's external leads and the voltage across the leads is simply the sum of the three subcells. For this cell at 1-sun, the individual subcell contributions to the overall V_{oc} are: GaInP: 1.440 V, GaAs: 1.020 V, and GaInAs: 0.640 V. If the middle-top R is equal to 1, any voltage increase will be the result of extra photocurrent in the bottom subcell at wavelengths between 900 and 1300 nm (see Figs. 1 and 2).

Photocurrent ratios can be quantified without spectral irradiance if the is spectral mismatches between isotype cells and their corresponding subcells are assumed to be unity (true if they have identical QEs). Figure 7 shows the results of measuring isotype I_{sc} ratios as the HIPSS PNV was varied through its entire range, where the vertical arrow shows the PNV at which the middle-top R is unity, PNV=372, and the horizontal arrow shows the ratios associated with the bottom at this condition, which are 1.34 (the bottom-top and bottom-middle ratios are always equal when the middle-top is unity because of how the ratios are defined).
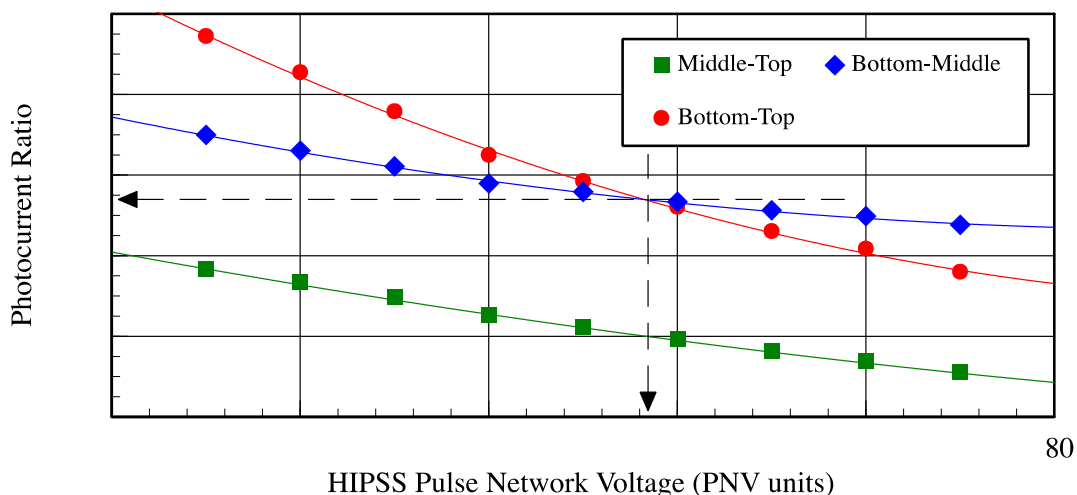

Figure 7. Photocurrent ratio versus HIPSS PNV for a GaInP/GaAs/GaInAs triple cell determined with isotype reference cells and assuming unity spectral mismatch.

Figure 7 also demonstrates that for any value of PNV, the HIPSS spectral irradiance is such that the bottom subcell will always generate photocurrents that are artificially high, regardless of the middle-top R.

10

3.3 Fill Factor Discontinuities

To demonstrate the effects of excess bottom irradiance, a numeric model was used to generate *FF* versus concentration for GaInAs- and Ge-based bottom subcells. The top and middle subcells were GaInP and GaAs with diode ideality factors (*n*) equal to one, and the bottom subcell ideality factors were two in both cases. A series resistance was chosen to simulate a reasonable roll-off at high concentration. These calculations are plotted in Fig. 8, where the solid curves correspond to photocurrents balanced with the direct reference spectrum, while the dashed curves have a 30% excess photocurrent in the bottom subcells to simulate the HIPSS measurement conditions.
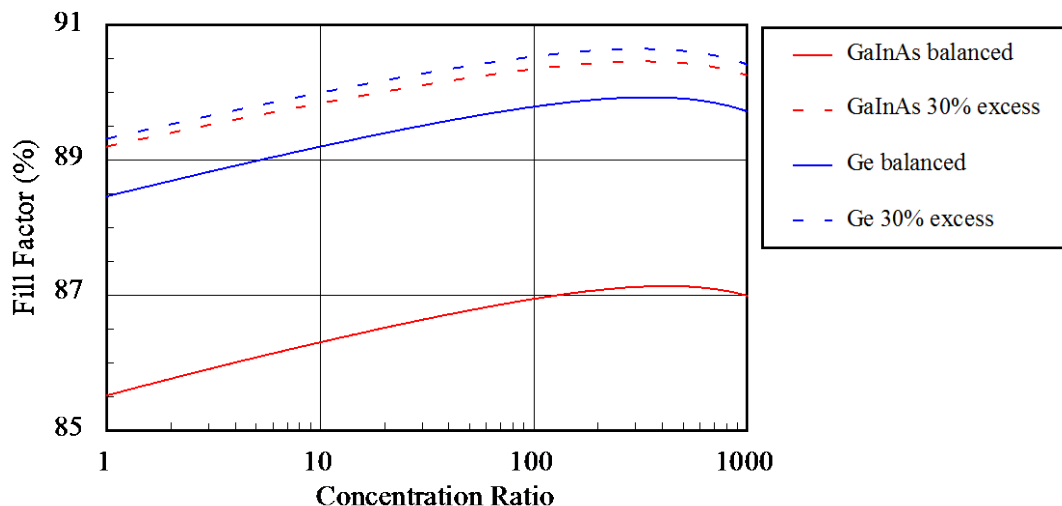

Figure 8. Modeled fill factor versus concentration ratio for two different triple cells, GaInP/GaAs/GaInAs and GaInP/GaAs/Ge.

This work demonstrates that: 1) *FF* versus concentration is predicted to be a smooth curve without discontinuities, 2) the discontinuities observed in GaInAs-based triple cells between the X-25 and HIPSS measurements can be reasonably explained by incorrect spectral irradiance, and 3) the effects of excess bottom-subcell photocurrents are much stronger in GaInAs bottom subcells compared with Ge subcells.

By taking advantage of the OSMSS's spectral adjustment capabilities, it is possible to measure how the *FF* varies with the excess irradiance. First, the simulator was adjusted to the reference spectrum at 1-sun for a GaInP/GaAs/GaInAs cell similar to the cell from which Fig. 6 was generated. Next, the OSMSS light source corresponding to the bottom subcell was varied from 70% to 140% and the I-V curve measured at each value. These data are plotted in Fig. 9. Note that as the bottom subcell increases above 100% the *FF* increases monotonically. Also, the I_{sc} is constant in this region, indicating either the top or middle is the limiting subcell, while the bottom subcell limits I_{sc} when its irradiance is reduced below 100%.

11
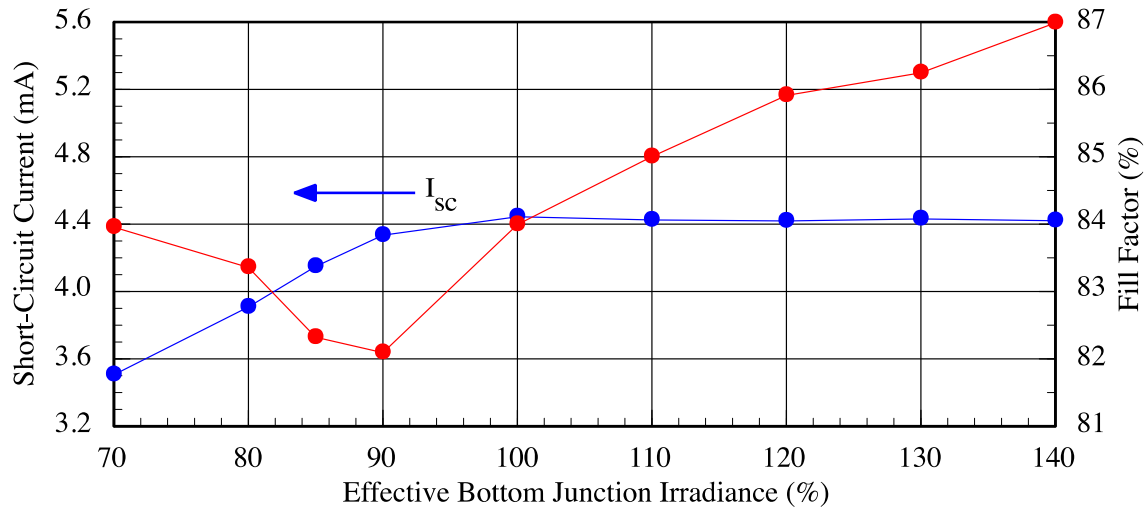
Figure 9. Short-circuit currant and fill factor versus bottom subcell irradiance for a GaInP/GaAs/GaInAs triple cell (OSMSS data).

3.4 Comparison of HIPSS and T-HIPSS Data

With the T-HIPSS, it is now possible to adjust the spectral irradiance so that the R values are within 1.00 ± 0.01 for triple cells and compare the I-V parameters against HIPSS data in which the bottom subcell is overdriven. In Fig. 10, the HIPSS data from Fig. 6 is compared with two separate T-HIPSS measurements on the same GaInP/GaAs/GaInAs cell; for one data set the spectral irradiance was adjusted until all three R-values were within ± 0.004 of unity, and for the second set light to the bottom subcell was increased until the bottom-top and bottom-middle R values were 1.45. Thus, this second set simulates light conditions in the HIPSS by overdriving the bottom subcell with 45% extra irradiance. It is evident that the T-HIPSS tuned data set agrees quite well with the OSMSS data when the trends are extrapolated down to 1-sun, while the other two sets show large offsets for the FF and η.

12
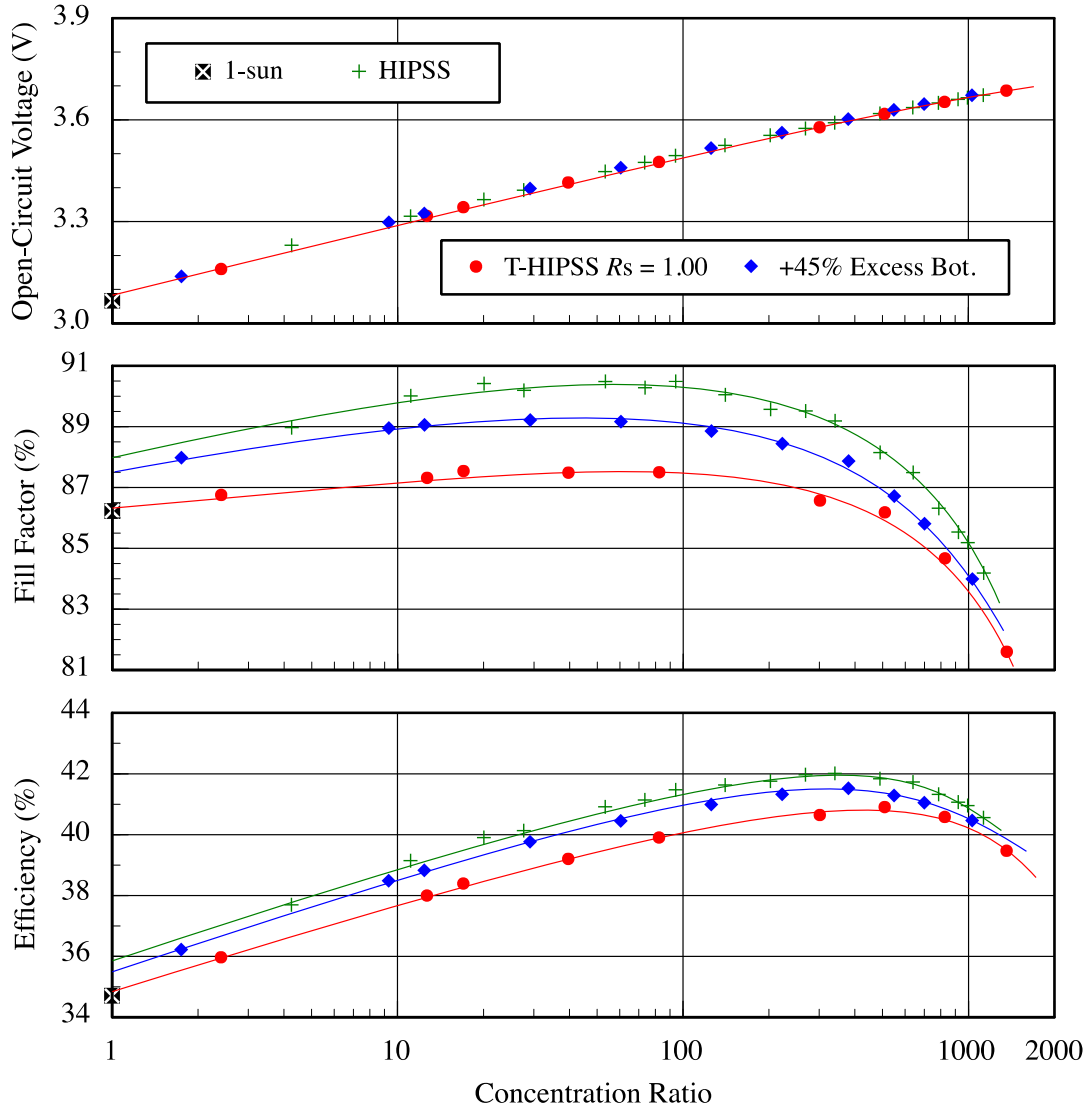
Figure 10. Comparison of I-V parameters versus concentration ratio for the triple cell from Fig. 6 (HIPSS and T-HIPSS data).

3.5 V$_{oc}$ Increases Due to Excess Subcell Photocurrents

Close examination of the T-HIPSS V_{oc} data in Fig. 10 reveals a constant offset of +10 mV from the tuned to the +45% excess bottom subcell conditions over the entire range of concentrations. From solar cell theory, a change of V_{oc} caused by a change of photocurrent in a single cell at 25°C can be expressed as [18]:

$$\Delta V_{oc} = 25.7\text{mV} \cdot n \cdot \left[\ln(\rho_1) - \ln(\rho_2) \right] = 25.7\text{mV} \cdot n \cdot \ln(R) \qquad (4)$$

Note that this change depends only on the diode quality factor and the photocurrent ratio, and isn't related to the bandgap. For a multijunction cell, the total change will be the sum from each subcell:

13

$$\Delta V_{oc} = 25.7\,\text{mV} \cdot \sum_{1}^{N} n_i \ln(R_i) \tag{5}$$

When only the bottom subcell irradiance is changed, Eq. 5 reduces back to Eq. 4. With ΔV_{oc} and R known, solving for the diode quality factor gives $n = 1.047$, a quite reasonable value.

It has been assumed that the spectral conditions in the HIPSS are such that the middle-top subcell R is correct, but this may not true. If this ratio is incorrect, then according the Eq. 5, the V_{oc} offset will include a contribution from the second subcell. Because the HIPSS FF and η in Fig. 10 are both higher than the T-HIPSS +45% bottom subcell curves, the HIPSS spectral conditions are likely farther away.

Looking at the V_{oc} plots in Fig. 10 again, three separate regions can be discerned. Above about 200×, the rate of change of V_{oc} with concentration is reduced, reaching a drop of about 20 mV at 1100×. This drop is likely caused by cell heating during the flash I-V measurement. Between 10× and 100× the increase with concentration is logarithmic, and a curve fit in this range indicates the n factor sum (see Eq. 5) is 3.30. Below 10× the change is still logarithmic, but the n factor sum has increased to 3.94.

3.6 Empirical Spectral Imbalance Data Correction Procedure

Figure 10 suggests the possibility of correcting concentrator performance data for the effects of a non-adjustable solar simulator, if a 1-sun data point obtained with a spectrally adjustable simulator is available. By assuming the shapes of the curves do not vary with spectral irradiance, constant offsets are subtracted from V_{oc} and η data; the offsets are calculated from logarithmic extrapolation down to 1-sun and subtracted from the 1-sun data points. Fill factors corresponding to the corrected V_{oc} and η data can then be calculated.

By applying the procedure to the HIPSS and T-HIPSS +45% bottom data in Fig. 10, the results can then be directly compared with the T-HIPSS tuned data; this comparison is shown in Fig. 11. The procedure used was:

- Calculate ΔV_{oc}. For the T-HIPSS we take advantage of the tuned data and apply the constant -10 mV offset, as discussed above. The HIPSS data, however, lacks data points below 4×, and extrapolating a logarithmic fit over the 4× to 30× range down to 1-sun gives a ΔV_{oc} of -38 mV. Because this offset would overcorrect and introduce error, no ΔV_{oc} was applied to the HIPSS data.

- Calculate $\Delta\eta$. These were done over the 2× to 40× range and gave -1.10% for the HIPSS data, and -0.86% for the T-HIPSS +45% bottom data.

- Calculate $V'_{oc} = V_{oc} - \Delta V_{oc}$ and $\eta' = \eta - \Delta\eta$ for each data point.

- Calculate the FF that corresponds to the corrected V_{oc} and η: $FF' = FF\left(\eta'/\eta\right)\left(V_{oc}/V'_{oc}\right)$.

The results of the data corrections are shown in Fig. 11.

14
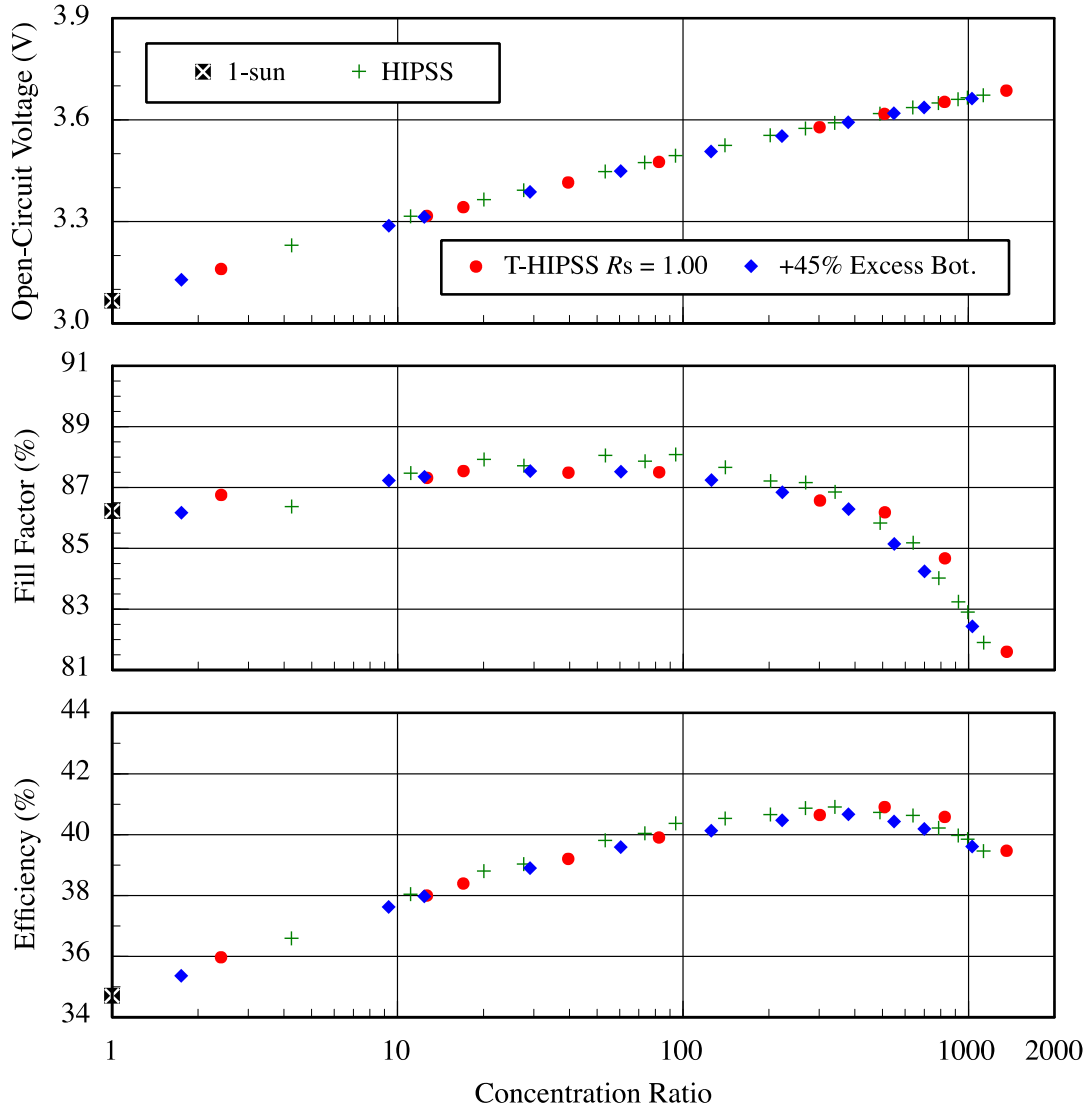
**Figure 11. Comparison of I-V parameters versus concentration ratio for the triple cell from Fig. 10, corrected for spectral imbalance (HIPSS and T-HIPSS data).**

4 Conclusions

Although it has been known for many years that accurate efficiency measurements of multijunction solar cells to SRC require spectrally adjustable solar simulation, extension of these measurement principles to high-efficiency concentrator cells has been hindered by the lack of capable I-V measurement systems. Specifically, high-speed acquisition of spectral irradiance data and independent spectral adjustment in sufficient wavelength bands for high intensity pulsed Xe simulators have not been available.

In general, the spectral content of unfiltered Xe flash lamps for IR wavelengths greater than 900 nm is too high due to the Xe emission lines. Measurement of GaInP/GaAs/Ge triple cells has been possible using such simulators, however, because the Ge bottom photocurrents were much higher than those of the top and middle subcells. Using this technique for Ge-based cells has been validated.

15

Newer triple cell designs with bottom subcells that respond to a narrower wavelength range are therefore much more sensitive to excess irradiance. The internal I-V characteristics of recent high-efficiency GaInP/GaAs/GaInAs cells combine to produce external I-V curves with inflated fill factors when illuminated with a raw Xe spectrum. This propagates as an error in the measured efficiency that is always too high.

A good rule-of-thumb based on our work is that any concentrator SRC efficiency measurement of a triple cell, in which the subcell photocurrents are comparable in magnitude, uses unfiltered Xe simulator illumination, and the fill factor exceeds 88 to 89% at high concentration, should be flagged and suspected of having excess bottom-subcell irradiance.

Lastly, this error can be avoided with proper spectrally adjustable measurement systems, such as the Spectrolab T-HIPSS and the OSMSS. If a spectrally adjustable concentrator simulator is not available, a correction procedure based on logarithmic extrapolation can be used to mitigate the effects of excess subcell irradiance, provided that a 1-sun data point from an adjustable simulator is available. This empirical correction can lose validity if the uncorrected I-V performance data do not include sufficient data points at low concentration.

While the error has been identified in GaInP/GaAs/GaInAs triple cells measured with unfiltered Xe-arc lamps, it should be emphasized that similar errors can arise whenever the photocurrent in a single subcell is artificially increased, regardless of the subcell's bandgap or semiconductor composition. Figure 8 demonstrates that it also occurs in Ge-based cells, although to a lesser degree. Increasing the photocurrent in a GaAs middle cell, for example, will also increase the measured efficiency.

References

[1] ASTM G 173–12 (2012). "Standard Tables for Reference Solar Spectral Irradiances: Direct Normal and Hemispherical on 37° Tilted Surface." *Annual Book of ASTM Standards* (14.04). West Conshohocken, PA: ASTM International.

[2] ASTM E 490–06 (2006). "Solar Constant and Air Mass Zero Solar Spectral Irradiance Tables." *Annual Book of ASTM Standards* (15.03). West Conshohocken, PA: ASTM International.

[3] Osterwald, C.R. (1986) "Translation of Device Performance Measurements to Reference Conditions." *Solar Cells* (18); pp. 269–279.

[4] Emery, K.A. (1986) "Solar Simulators and I-V Measurement Methods." *Solar Cells* (18); pp. 251–260.

[5] ASTM E 948–09 (2009). "Standard Test Method for Electrical Performance of Photovoltaic Cells Using Reference Cells Under Simulated Sunlight." *Annual Book of ASTM Standards* (12.02). West Conshohocken, PA: ASTM International.

[6] Emery, K. (2011). "Measurement and Characterization of Solar Cells and Modules." *Handbook of PV Sci. and Eng., 2nd Ed.* (7). Ch. 18; pp. 797-840. John Wiley & Sons, W. Sussex, UK, ISBN -0-470-72169-8.

[7] ASTM E 973–10 (2010). "Standard Test Method for Determination of the Spectral Mismatch Parameter Between a Photovoltaic Device and a Photovoltaic Reference Cell." *Annual Book of ASTM Standards* (12.02). West Conshohocken, PA: ASTM International.

[8] Wanlass, M.W.; Albin, D.S. (2004). "Rigorous Analysis of Series-Connected, Multi-Bandgap, Tandem Thermophotovoltaic (TPV) Energy Converters." *Proc. 6th Conf. on Thermophotovoltaic Gen. of Electricity*, Freiburg, Germany; AIP Conference Proceedings (738); pp. 462-470.

[9] McMahon, W.E.; Emery, K.E.; Friedman, D.J.; Ottoson, L.; Young, M.S.; Ward, J.S.; Kramer, C.M.; Duda, A.; Kurtz, S. (2008). "Fill Factor as a Probe of Current-Matching for $GaInP_2$/GaAs Tandem Cells in a Concentrator System During Outdoor Operation." *Prog. in PV: Res. Appl.* (16); pp. 213-224.

[10] Burdick, J.; Glatfelter, T. (1986) "Spectral Response and I-V Measurements of Tandem Amorphous-Silicon Alloy Solar Cells." *Solar Cells* (18); pp. 310–314.

[11] Emery, K.A.; Osterwald, C.R.; Glatfelter, T.; Burdick, J.; Virshup G., (1988). "A Comparison of the Errors in Determining the Efficiency of Multijunction Solar Cells by Various Methods." *Solar Cells* (24); pp. 371-380.

[12] Virshup G.F. (1990). "Measurement Techniques for Multijunction Solar Cells." *Proc. 21st IEEE PV Spec. Conf.*, Kissimimee, FL; pp.1249-1255.

[13] Nagamine, F.; Shimokawa, R.; Suzuki, M.; Abe, T. (1993). "New Solar Simulator for Multi-Junction Solar Cell Measurements." *Proc. 23rd IEEE PV Spec. Conf.*, Louisville, KY; pp. 686-690.

[14] Emery, K.; Meusel, M.; Beckert, R.; Dimroth, F.; Bett, A.; Warta, W. (2000) "Procedures for Evaluating Multijunction Concentrators," *Proc. 28th IEEE Photovoltaic Specialists Conf.*, Anchorage, AL; pp. 1126-1130.

[15] ASTM E 2236–10 (2010). "Standard Test Methods for Measurement of Electrical Performance and Spectral Response of Nonconcentrator Multijunction Photovoltaic Cells and Modules." *Annual Book of ASTM Standards* (12.02). West Conshohocken, PA: ASTM International.

[16] Moriarty, T.; Jablonski, J,; Emery, K. (2012). "Algorithm for Building a Spectrum for NREL One-Sun Multi-Source Simulator." *Proc. 38th IEEE Photovoltaic Specialists Conf.*, Austin, TX.

[17] Kiehl, J.; Emery, K.; Andreas, A. (2004). "Testing Concentrator Cells: Spectral Considerations of a Flash Lamp System," *Proc. 19th Euro. PV Sol. Energy Conf. and Exhibition*, Paris France; 5BV.2.11.

[18] Green, M.A. (1995),"Silicon Solar Cells: Advanced Principles and Practice." Univ. of New South Wales, Sydney, Australia.